Molecular picture for $X_0(2900)$ and $X_1(2900)$*

Jun He(何军)[1†] Dian-Yong Chen(陈殿勇)[2‡]

[1]Department of Physics and Institute of Theoretical Physics, Nanjing Normal University, Nanjing 210097, China
[2]School of Physics, Southeast University, Nanjing 210094, China

Abstract: Inspired by the newly observed $X_0(2900)$ and $X_1(2900)$ at LHCb, the $K^*\bar{D}^*$ and $K\bar{D}_1$ interactions are studied in the quasipotential Bethe-Salpeter equation approach combined with the one-boson-exchange model. The bound and virtual states from the interactions are searched for as the poles in the complex energy plane of scattering amplitude. A bound state with $I(J^P)=0(0^+)$ and a virtual state with $0(1^-)$ are produced from the $K^*\bar{D}^*$ interaction and $K\bar{D}_1$ interaction, and can be related to the $X_0(2900)$ and $X_1(2900)$ observed at LHCb, respectively. A bound state with $I(J^P)=0(1^+)$ and a virtual state with $I(J^P)=0(2^+)$ are also predicted from the $K^*\bar{D}^*$ interaction with the same α value to reproduce the $X_{0,1}(2900)$, which can be searched for in future experiments.

Keywords: molecular state, quasipotential Bethe-Salpeter equation, potential model

DOI:

I. INTRODUCTION

In the past decades, a growing number of new hadron states have been observed experimentally, then the investigations on the nature of these new hadron states have become one of intriguing topic in hadron physics. Among these new hadron states, some are hardly assigned as conventional mesons or baryons, thus they were considered as good candidates of QCD exotic states, such as hadronic molecular states, compact multiquark states and hybrid states (for recent reviews, we refer to Refs. [1-11]).

Very recently, the LHCb collaboration observed two new states, $X_0(2900)$ and $X_1(2900)$, in the K^+D^- invariant mass distribution of $B^+\to D^+D^-K^+$, the resonance parameters of these two states were reported to be [12],

$$\begin{aligned} m_{X_0(2900)} =&(2866\pm7)\ \text{MeV},\\ \Gamma_{X_0(2900)} =&(57.2\pm12.9)\ \text{MeV},\\ m_{X_1(2900)} =&(2904\pm5)\ \text{MeV},\\ \Gamma_{X_1(2900)} =&(110.3\pm11.5)\ \text{MeV}, \end{aligned} \tag{1}$$

respectively. The J^P quantum numbers of $X_0(2900)$ and $X_1(2900)$ are 0^+ and 1^-, respectively [12].

Since $X_0(2900)$ and $X_1(2900)$ are observed in the K^+D^- channel, the only possible quark components of these states are $ud\bar{c}\bar{s}$, which indicates that they are composed of quarks with four different flavors. Such kind of states are particularly interesting since they obviously can not be assigned as a conventional hadron. Actually, in 2016 another similar structure $X(5568)$ was reported by the D0 collaboration in the $B_s\pi$ invariant mass distribution, which is also a fully open flavor state [13]. However, after the observation of D0 collaboration, the LHCb, CMS, CDF, and ATLAS Collaborations negated the existence of $X(5568)$ [14-17]. Thus, the present observation of $X_0(2900)$ and $X_1(2900)$ brings physicists' attentions back to the existence of fully open flavor states again.

Considering four different flavor quark components of $X_0(2900)$ and $X_1(2900)$, one can naturally consider these states as tetraquark candidates. In Ref. [18], the mass spectrum of exotic tetraquark states with four different flavors is investigated by using a color-magnetic interaction model, where the masses of states with $I(J^P)=1(0^+)$ were 2607 and 3129 MeV, while those with $I(J^P)=0(0^+)$ were 2320 and 2850 MeV. After the observation of $X_0(2900)$ and $X_1(2900)$, the authors in Refs. [19, 20] indicated that the $X_0(2900)$ can be an isosinglet compact tetraquark state, while the estimations in Ref. [21] indicates that the $X_0(2900)$ should be a radial excited tetraquark with $J^P=0^+$. As for $X_0(2900)$, the investigations in Refs. [21, 22] support that the $X_1(2900)$ can be as-

Received 6 January 2021; Accepted 11 March 2021

* Supported by the National Natural Science Foundation of China (11675228, 11775050), and the Fundamental Research Funds for the Central Universities

† E-mail: junhe@njnu.edu.cn
‡ E-mail: chendy@seu.edu.cn

signed as a P-wave compact diquark-antidiquark tetraquark state. However, the calculaions in an extended relativized quark model indicate that the predicted mass of 0^+ $ud\bar{s}\bar{c}$ are different from that of the $X_0(2900)$, which disfavors the assignment of the $X_0(2900)$ as a compact tetraquark [23].

It should be noticed that in the vicinity of 2900 MeV, there are abundant thresholds of a charmed and a strange mesons, such as K^*D^*, KD_1, KD_0. In Refs. [24, 25], the possible molecular states composed of (anti-)charmed and strange mesons have been investigated. Considering the J^P quantum numbers of $X_0(2900)$ and $X_1(2900)$, the former one can be resulted from the $K^*\bar{D}^*$ interaction, while the latter one can be resulted from the $K\bar{D}_1$ interaction. In Ref. [26], the structure corresponding to $X_0(2900)$ and $X_1(2900)$ can be interpreted as the triangle singularity. While in Ref. [27], the estimation in one-boson exchange model indicates that the interaction of $K^*\bar{D}^*$ are strong enough to form a molecular state, thus, $X_0(2900)$ can be interpreted as a $K^*\bar{D}^*$ molecular state and such an interpretation was also supported by the estimations in Refs. [22, 28].

Along the way of molecular interpretations, we construct the one-boson-exchange potential of $K^*\bar{D}^*$ and $K\bar{D}_1$ interactions. The scattering amplitude can be obtained with the help of the quasipotential Bethe-Salpeter equation (qBSE) from the interaction potentials, and the poles of the scattering amplitudes are searched in complex energy plane. In the current work, both bound and virtual states will be considered in the calculation to discuss the relation between experimentally observed states $X_0(2900)/X_1(2900)$ and the $K^*\bar{D}^*/K\bar{D}_1$ interactions.

This work is organized as follows. We present the formalism used in the present estimation in the following section. The numerical results and related discussions are given in section III and the last section is devoted to a short summary.

II. FORMALISM

In the current work, we will consider two interactions, $K^*\bar{D}^*$ and $K\bar{D}_1$ interactions. The possible isospins of the states composed by $K^*\bar{D}^*$ and $K\bar{D}_1$ could be 0 and 1, and the corresponding flavor functions are

$$
\begin{aligned}
|K^*\bar{D}^*, I=0\rangle &= \frac{1}{\sqrt{2}}\left[K^{*+}D^{*-} - K^{*0}\bar{D}^{*0}\right],\\
|K^*\bar{D}^*, I=1\rangle &= \frac{1}{\sqrt{2}}\left[K^{*+}D^{*-} + K^{*0}\bar{D}^{*0}\right],\\
|K\bar{D}_1, I=0\rangle &= \frac{1}{\sqrt{2}}\left[K^{+}D_1^{-} - K^{0}\bar{D}_1^{0}\right],\\
|K\bar{D}_1, I=1\rangle &= \frac{1}{\sqrt{2}}\left[K^{+}D_1^{-} + K^{0}\bar{D}_1^{0}\right],
\end{aligned} \tag{2}
$$

respectively.

In the one-boson-exchange model, the K^* meson and $\bar{D}^*$ meson interact by exchanging π, η, ρ, and ω mesons. For the $K\bar{D}_1$ interaction, the π and η exchanges are forbidden, only vector exchanges are allowed. Here, the vector exchanges are included explicitly, so we do not consider the contact terms as discussed in Ref. [29-33]. To describe the interaction, we need the effective Lagrangians at two vertices. For the charmed meson part, the effective Lagrangians can be written with the help of heavy quark and chiral symmetries as [34-38],

$$
\begin{aligned}
\mathcal{L}_{\mathcal{P}^*\mathcal{P}^*\mathbb{P}} &= \frac{2g}{f_\pi}\epsilon_{\mu\nu\alpha\beta}\tilde{\mathcal{P}}_a^{*\mu}\tilde{\mathcal{P}}_b^{*\nu\dagger}v^\alpha\partial^\beta\mathbb{P}_{ba},\\
\mathcal{L}_{\mathcal{P}^*\mathcal{P}^*\mathbb{V}} &= -\sqrt{2}\beta g_V\tilde{\mathcal{P}}^*_a\cdot\tilde{\mathcal{P}}_b^{*\dagger}\,v\cdot\mathbb{V}_{ba}\\
&\quad + i2\sqrt{2}\lambda g_V\tilde{\mathcal{P}}_a^{*\mu}\tilde{\mathcal{P}}_b^{*\nu\dagger}(\partial_\mu\mathbb{V}_\nu-\partial_\nu\mathbb{V}_\mu)_{ba},\\
\mathcal{L}_{\mathcal{P}_1\mathcal{P}_1\mathbb{V}} &= -\sqrt{2}\beta_2 g_V\tilde{\mathcal{P}}_{1a}\cdot\tilde{\mathcal{P}}_{1b}^{\dagger}\,v\cdot\mathbb{V}_{ba}\\
&\quad - \frac{5\sqrt{2}i\lambda_2 g_V}{3}\tilde{\mathcal{P}}_{1a}^{\mu}\tilde{\mathcal{P}}_{1b}^{\nu\dagger}(\partial_\mu\mathbb{V}_\nu-\partial_\nu\mathbb{V}_\mu)_{ba},
\end{aligned} \tag{3}
$$

where the velocity v should be replaced by $i\overleftrightarrow{\partial}/\sqrt{m_i m_f}$ with the $m_{i,f}$ being the mass of the initial or final heavy meson. The $\tilde{\mathcal{P}}=(\bar{D}^0, D^-, D_s^-)$ and $\tilde{\mathcal{P}}^*=(\bar{D}^{*0}, D^{*-}, D_s^{*-})$ satisfy the normalization relations $\langle 0|\tilde{\mathcal{P}}|\bar{Q}q(0^-)\rangle=\sqrt{M_{\tilde{\mathcal{P}}}}$ and $\langle 0|\tilde{\mathcal{P}}^*_\mu|\bar{Q}q(1^-)\rangle=\epsilon_\mu\sqrt{M_{\tilde{\mathcal{P}}^*}}$. The $\mathbb{P}$ and $\mathbb{V}$ are the pseudoscalar and vector matrices as

$$
\begin{aligned}
\mathbb{P} &= \begin{pmatrix} \frac{\sqrt{3}\pi^0+\eta}{\sqrt{6}} & \pi^+ & K^+\\ \pi^- & \frac{-\sqrt{3}\pi^0+\eta}{\sqrt{6}} & K^0\\ K^- & \bar{K}^0 & -\frac{2\eta}{\sqrt{6}} \end{pmatrix},\\
\mathbb{V} &= \begin{pmatrix} \frac{\rho^0+\omega}{\sqrt{2}} & \rho^+ & K^{*+}\\ \rho^- & \frac{-\rho^0+\omega}{\sqrt{2}} & K^{*0}\\ K^{*-} & \bar{K}^{*0} & \phi \end{pmatrix},
\end{aligned} \tag{4}
$$

which correspond to $(\bar{D}^0, D^-, D_s^-)$. The coupling constants have been determined in the literature with the heavy quark symmetry and available experimental data, i.e., $g=0.59$, $\beta=0.9$, $\lambda=0.56$, $\beta_2=1.1$, $\lambda_2=-0.6$, with $g_V=5.9$ and $f_\pi=0.132$ GeV [39-44].

To describe the couplings of the $K^{(*)}$ meson with exchanged pseudoscalar and/or vector mesons, the effective Lagrangians are adopted as

$$
\mathcal{L}_{KKV} = -ig_{KKV}\,KV^\mu\partial_\mu K + \text{H.c.},
$$

$$\begin{aligned}\mathcal{L}_{K^*K^*V} =& \mathrm{i}\frac{g_{K^*K^*V}}{2}(K^{*\mu\dagger}V_{\mu\nu}K^{*\nu}+K^{*\mu\nu\dagger}V_{\mu}K^{*\nu}\\&+K^{*\mu\dagger}V_{\nu}K^{*\nu\mu}),\\ \mathcal{L}_{K^*K^*P} =& g_{K^*K^*P}\epsilon^{\mu\nu\sigma\tau}\partial^{\mu}K^{*\nu}\partial_{\sigma}PK^{*\tau}+\mathrm{H.c.},\end{aligned} \quad (5)$$

where $K^{*\mu\nu}=\partial^{\mu}K^{*\nu}-\partial^{\nu}K^{*\mu}$. The flavor structures are $K^{*\dagger}A\cdot\boldsymbol{\tau}K^*$ for an isovector A $(=\pi$ or $\rho)$ meson, and $K^{*\dagger}K^*B$ for an isoscalar B $(=\eta,\ \omega)$ meson. With the help of the $SU(3)$ symmetry, the coupling constants can be obtained from the $\rho\rho\rho$ and $\rho\omega\pi$ couplings. The $g_{\rho\rho\rho}$ was suggested equivalent to $g_{\pi\pi\rho}=6.2$, and $g_{\omega\pi\rho}=11.2$ GeV^{-1} [45-47]. The $SU(3)$ symmetry suggests $g_{K^*K^*\rho}=g_{K^*K^*\omega}=g_{\rho\rho\rho}/(2\alpha)$, and $g_{K^*K^*\pi}=g_{K^*K^*\eta}/[-\sqrt{1/3}(1-4\alpha)]=g_{\omega\rho\pi}/(2\alpha)$ with $\alpha=1$ [48-51].

In fact, the above vertices has been applied to study many XYZ particles and hidden-strange molecular states [44, 49-54]. Hence, in the current work, we only need to reconstruct the vertices $\Gamma_{1,2}$ for charmed or strange mesons to the potential considered here as

$$\mathcal{V}_{\mathbb{P}}=I_{\mathbb{P}}\Gamma_1\Gamma_2P_{\mathbb{P}}f_{\mathbb{P}}^2(q^2),\quad \mathcal{V}_{\mathbb{V}}=I_{\mathbb{V}}\Gamma_{1\mu}\Gamma_{2\nu}P_{\mathbb{V}}^{\mu\nu}f_{\mathbb{V}}^2(q^2), \quad (6)$$

where the propagators are defined as usual as

$$P_{\mathbb{P}}=\frac{\mathrm{i}}{q^2-m_{\mathbb{P}}^2},\quad P_{\mathbb{V}}^{\mu\nu}=\mathrm{i}\frac{-g^{\mu\nu}+q^{\mu}q^{\nu}/m_{\mathbb{V}}^2}{q^2-m_{\mathbb{V}}^2}, \quad (7)$$

and we adopt a form factor $f_{\mathbb{P},\mathbb{V}}(q^2)$ to compensate the off-shell effect of exchanged meson as $f_e(q^2)=\mathrm{e}^{-(m_e^2-q^2)^2/\Lambda_e^2}$ with m_e being the $m_{\mathbb{P},\mathbb{V}}$ and q being the momentum of the exchanged meson. Such treatment also reflects the non-pointlike nature of the constituent mesons. The cutoff is rewritten as a form of $\Lambda_e=m_e+\alpha_e\,\Lambda_{\rm QCD}$ with $\Lambda_{\rm QCD}$ being the scale of QCD and taking as 0.22 GeV [55]. The flavor factors $I_{\mathbb{P},\mathbb{V}}$ for certain meson exchange and total isospin are presented in Table 1.

With the potential, the scattering amplitude can be obtained with the qBSE [56-58]. The qBSE with fixed spin-parity J^P is written as [29, 50, 59],

$$\begin{aligned}\mathrm{i}\mathcal{M}^{J^P}_{\lambda'\lambda}(p',p)=&\mathrm{i}\mathcal{V}^{J^P}_{\lambda',\lambda}(p',p)+\sum_{\lambda''}\int\frac{p''^2\mathrm{d}p''}{(2\pi)^3}\\&\times\mathrm{i}\mathcal{V}^{J^P}_{\lambda'\lambda''}(p',p'')G_0(p'')\mathrm{i}\mathcal{M}^{J^P}_{\lambda''\lambda}(p'',p),\end{aligned} \quad (8)$$

Table 1. The flavor factors $I_{\mathbb{P},\mathbb{V}}$ for certain meson exchange and total isospin. The π and η exchanges are forbidden for $K\bar{D}_1$ interaction.

	I_π	I_η	I_ρ	I_ω
$I=0$	$-3\sqrt{2}/2$	$1/\sqrt{6}$	$-3\sqrt{2}/2$	$1\sqrt{2}$
$I=1$	$\sqrt{2}/2$	$1/\sqrt{6}$	$\sqrt{2}/2$	$1/\sqrt{2}$

where the sum extends only over nonnegative helicity λ''. The $G_0(p'')$ is reduced from 4-dimensional propagator by the spectator approximation, and in the center-of-mass frame with $P=(W,\mathbf{0})$ it reads,

$$G_0(p'')=\frac{1}{2E_h(p'')[(W-E_h(p''))^2-E_l^2(p'')]}. \quad (9)$$

Here, as required by the spectator approximation, the heavier meson $(h=\bar{D}^*,\bar{D}_1)$ is on shell, which satisfies $p_h''^0=E_h(p'')=\sqrt{m_h^2+p''^2}$. The $p_l''^0$ for the lighter meson $(l=K^*,K)$ is then $W-E_h(p'')$. A definition $p=|\boldsymbol{p}|$ will be adopted here. The partial-wave potential is defined with the potential of the interaction obtained in the above as

$$\begin{aligned}\mathcal{V}^{J^P}_{\lambda'\lambda}(p',p)=&2\pi\int\mathrm{d}\cos\theta\,[d^J_{\lambda\lambda'}(\theta)\mathcal{V}_{\lambda'\lambda}(\boldsymbol{p}',\boldsymbol{p})\\&+\eta d^J_{-\lambda\lambda'}(\theta)\mathcal{V}_{\lambda'-\lambda}(\boldsymbol{p}',\boldsymbol{p})],\end{aligned} \quad (10)$$

where $\eta=PP_1P_2(-1)^{J-J_1-J_2}$ with P and J being parity and spin for system, K^*/K meson or $\bar{D}^*/\bar{D}_1$ meson. The initial and final relative momenta are chosen as $\boldsymbol{p}=(0,0,p)$ and $\boldsymbol{p}'=(p'\sin\theta,0,p'\cos\theta)$. The $d^J_{\lambda\lambda'}(\theta)$ is the Wigner d-matrix. In the qBSE approach, a form factor will be introduced into the propagator to reflect the off-shell effect as an exponential regularization, $G_0(p)\to G_0(p)[\mathrm{e}^{-(k_1^2-m_1^2)^2/\Lambda_r^4}]^2$, where the k_1 and m_1 are the momentum and the mass of the strange meson. The cutoff Λ_r is also parameterized as in the Λ_e case. The α_e and α_r play analogous roles in the calculation of the binding energy. Hence, we take these two parameters as a parameter α for simplification [44]. Such parameter is also used to absorb the uncertainties of our model, such as the inaccuracy of heavy quark and $SU(3)$ symmetries in the Lagrangians.

III. NUMERICAL RESULTS AND DISCUSSION

The scattering amplitude obtained above is with the variation of the energy of system W. After continuation of the W to a complex energy z, the pole can be searched for in the complex energy z plane. The bound state corresponds to a pole at the real axis under threshold in the first Riemann sheet. If the attraction becomes weaker, the pole will move to the real axis under threshold in the second Riemann sheet, which corresponds to a virtual state [60]. In the current work, we will consider both bound and virtual states from the $K^*\bar{D}^*$ and $K\bar{D}_1$ interactions.

A. States from $K^*\bar{D}^*$ interaction

In the current work, we will consider six states from the $K^*\bar{D}^*$ interaction with isospin $I=(0,1)$, spin $J=(0,1,2)$, and parity $P=+$ which can be obtained in S wave. In our model, the only free parameter is the α in cutoff. Usually, small value of α should be chosen. For a cutoff Λ smaller than 3 GeV, the α should be smaller than 10. In the following, we present the results with α value in a larger range from 1 to 20 for discussion. We would like to remind in advance that the results with very large α are unreliable because it corresponds to a very small radius of the constituent hadrons. The results for the states from the $K^*\bar{D}^*$ interaction are presented and compared with experimentally observed $X_0(2900)$ in Fig. 1 (here we call the deviation between the pole of a virtual state and threshold as virtual energy).

Among the six states considered in the current work, four bound states can be produced from the $K^*\bar{D}^*$ interaction in the large range of α considered here. The bound states with $I(J^P)=0(0^+)$ and $0(1^+)$ appear at small α, about 4, and two bound states with 2^+ are found at α larger than 10. Usually, larger cutoff corresponds to stronger interaction, which leads to larger binding energy for a bound state. One can find that the binding energies of the four bound states increase with the increase of the α value.

Here, we also consider the possible virtual state from the interaction. Different from bound state, virtual state leaves the threshold further with the decreasing of α and weakening of attraction. The bound state with $I(J^P)=0(2^+)$ appears at α about 10, and the energy increases rapidly with the increase of the α value. However, if we reduce the α value, a pole can be found at second Riemann sheet, and leaves the threshold with the decrease of α value. The pole moves to a position about 40 MeV below the threshold at an α about 2, and disappears there. No virtual state can be found for the case with $0(0^+)$ and $1(2^+)$ if we reduce the α value. For $0(1^+)$ case, virtual state is also found, but disappears very rapidly with the decrease of α value.

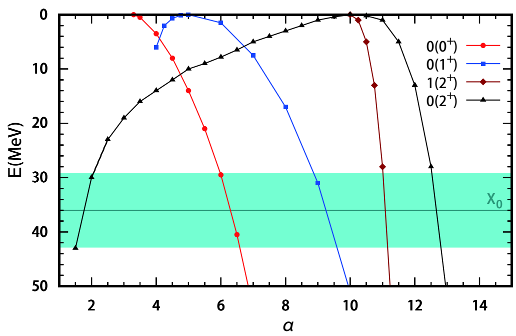

Fig. 1. (color online) The binding or virtual energy E of the bound or virtual states from the $K^*\bar{D}^*$ interaction with the variation of α. Here the $E=M_{th}-W$ with the M_{th} and W being the threshold and mass of the state. The circle, square, diamond, and triangle are for the states with $I(J^P)=0(0^+)$, $0(1^+)$, $1(2^+)$, and $0(2^+)$, respectively. The lines with cyan bar are for experimental mass and uncertainties of $X_0(2900)$ state, respectively.

Among the four bound states produced from the $K^*\bar{D}^*$ interaction, two bound states with $0(0^+)$ and $0(1^+)$ require small α value. For the $0(2^+)$ state, only virtual state can be produced with small α value. Since the $X_0(2900)$ and $X_1(2900)$ were observed in the K^+D^- channel, allowed quantum numbers of are 0^+ and 1^-. Hence, the current results support the assignment of the $X_0(2900)$ observed at LHCb as a $0(0^+)$ state from the $K^*\bar{D}^*$ interaction. As shown in Fig. 1, the experimental mass of the $X_0(2900)$ can be reproduced at an α of about 6. With such value of the α, the bound state with $0(1^+)$ and virtual state with $0(2^+)$ can be also produced from the $K^*\bar{D}^*$ interaction.

B. States from $K\bar{D}_1$ interaction

The $X_1(2900)$ state can not be reproduced from the $K^*\bar{D}^*$ interaction in S wave. Here we consider another system with a threshold close to the mass of $X_1(2900)$, the $K\bar{D}_1$ interaction. We will consider two states from the $K\bar{D}_1$ interaction with $I=(0,1)$ and $J^P=1^-$, which can be obtained in S wave. The results are presented in Fig. 2.

Among these two states, only the isoscalar interaction is attractive. However, the bound state with $0(1^-)$ appears at a very larger α value, about 16, which corresponds to a large cutoff Λ about 4 GeV. It is unreliable to assign the $X_1(2900)$ as a bound state. As the $0(2^+)$ state of the K^*D^* interaction, if we decrease the α value, a virtual state with $0(1^-)$ from the $K\bar{D}_1$ interaction can be found in a large range of the α from about 4 to 16. Such state can be related to the experimentally observed $X_1(2900)$. To reproduce the experimental mass of $X_1(2900)$, the value of the α should be chosen as about 6, which is also the value to reproduce the $X_0(2900)$.

IV. SUMMARY

In the current work, inspired by the newly observed $X_{0,1}(2900)$ at LHCb, the $K^*\bar{D}^*$ and $K\bar{D}_1$ interactions,

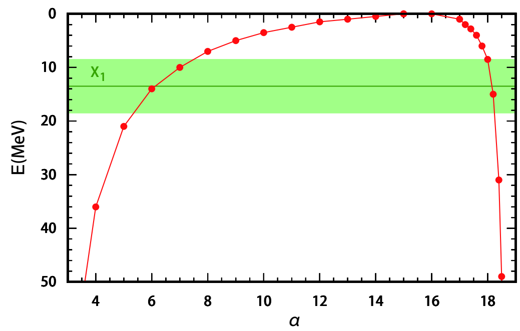

Fig. 2. (color online) The virtual or binding energy E of the bound or virtual state from the $K\bar{D}_1$ interaction with the variation of α. The circle is for the state with $I(J^P)=0(1^-)$. The lines with lightgreen bar are for experimental mass and uncertainties of $X_1(2900)$ state, respectively. Other conventions are the same as in Fig. 1.

which have thresholds about 2900 MeV, are studied in the qBSE approach. The bound and virtual states from the interaction are searched for as poles in the complex energy plane of the scattering amplitude, which is obtained from the one-boson-exchange potential.

A bound state with $0(0^+)$ is produced from the $K^*\bar{D}^*$ interaction. The radius R of the bound state state can be estimated as $R\sim 1/\sqrt{2\mu E_B}$ with μ and E_B being the reduced mass and binding energy [7]. The experimental binding energy, about 35 MeV, leads to a radius about 1 fm of the $K^*\bar{D}^*$ bound state. Considering the constituent mesons have radii about 0.5 fm, it supports the assignment of $X_0(2900)$ as a $K^*\bar{D}^*$ molecular state. The state with $0(0^+)$ from the $K^*\bar{D}^*$ interaction was suggested in many different approaches [22, 27, 28, 61].

A virtual state with $0(1^-)$ is also produced from the $K\bar{D}_1$ interaction with reasonable parameter. Different from the assignment of $X_0(2900)$ as a $K^*\bar{D}^*$ state with $0(0^+)$, the interpretation of $X_1(2900)$ is in the debate in the literature. In Ref. [62], a molecular state can be produced from the $K\bar{D}_1$ interaction by solving Bethe-Salpeter equation. In Ref. [22], the $X_1(2900)$ was interpreted as the P-wave $\bar{c}\bar{s}ud$ compact tetraquark state with 1^-. In Ref. [27], the $X_1(2900)$ can not be explained as a molecular state from the interaction considered.

These two states can decay into the K^+D^- channel in S and P waves, so can be related the $X_0(2900)$ and $X_1(2900)$ observed at LHCb, respectively. The $X_0(2900)$ states as an $K^*\bar{D}^*$ molecular state should be prone to separate to K^* and $\bar{D}^*$ mesons. Considering the K^* and $\bar{D}^*$ have decay widths of about 50 and <2 MeV, which provides a width of about 50 MeV to the $X_0(2900)$, which is quite close to the experimental value. For the $X_1(2900)$ states, the current study suggests that it is a virtual state. The virtual state is in the second Riemann sheet, which leads to a cusp at threshold, which may correspond to a larger width if we assume it as a resonance, which is also consistent with the experimental value larger than 100 MeV.

Besides these two states, a bound state with $0(1^+)$ and a virtual state with $0(2^+)$ are produced from the $K^*\bar{D}^*$ interaction with a small α value, about 6, which is also the value to reproduce the $X_{0,1}(2900)$. The mass order of the $0(0^+)$ and $0(1^+)$ states predicted in Ref. [27] is consistent with our results, and in both models, very large cutoff is required to produce a $0(2^+)$ bound state. In Ref. [28], masses of 2.722, 2.866 GeV for $0(1^+)$ state, and 2.866 GeV for $0(2^+)$ state were predicted with the $X_0(2900)$ as input. In Ref. [61], different mass order was predicted as 2866, 2861, and 2775 MeV for $0(0^+)$, $0(1^+)$, and $0(2^+)$, respectively, which follows their previous work in Ref. [25]. The low mass of 2^+ state was also found in the studies of f_J and D_J mesons [63, 64]. Such explicit difference in the mass order may be from the explicit form and treatment of the interaction. More theoretical research and experimental search of such states, especially the mass order of these states, are helpful to understand the $X(2900)$.

References

[1] H. X. Chen, W. Chen, X. Liu *et al.*, Phys. Rept. **639**, 1 (2016)
[2] A. Hosaka, T. Iijima, K. Miyabayashi *et al.*, PTEP **2016**, 062C01 (2016)
[3] J. M. Richard, Few Body Syst. **57**, 1185 (2016)
[4] R. F. Lebed, R. E. Mitchell, and E. S. Swanson, Prog. Part. Nucl. Phys. **93**, 143-194 (2017)
[5] A. Ali, J. S. Lange, and S. Stone, Prog. Part. Nucl. Phys. **97**, 123-198 (2017)
[6] A. Esposito, A. Pilloni, and A. Polosa, Phys. Rept. **668**, 1-97 (2017)
[7] F. K. Guo, C. Hanhart, U. G. Meißner *et al.*, Rev. Mod. Phys. **90**, 015004 (2018)
[8] S. L. Olsen, T. Skwarnicki, and D. Zieminska, Rev. Mod. Phys. **90**, 015003 (2018)
[9] M. Karliner, J. L. Rosner, and T. Skwarnicki, Ann. Rev. Nucl. Part. Sci. **68**, 17 (2018)
[10] Y. R. Liu, H. X. Chen, W. Chen *et al.*, Prog. Part. Nucl. Phys. **107**, 237 (2019)
[11] N. Brambilla, S. Eidelman, C. Hanhart *et al.*, arXiv:1907.07583
[12] LHC Seminar, by Daniel Johnson, CERN, August 11, 2020, https://indico.cern.ch/event/900975/
[13] V. M. Abazov *et al.*, Phys. Rev. Lett. **117**(2), 022003 (2016)
[14] T. Aaltonen *et al.*, Phys. Rev. Lett. **120**(20), 202006 (2018)
[15] M. Aaboud *et al.*, Phys. Rev. Lett. **120**(20), 202007 (2018)
[16] A. M. Sirunyan *et al.*, Phys. Rev. Lett. **120**(20), 202005 (2018)
[17] R. Aaij *et al.*, Phys. Rev. Lett. **117**(15), 152003 (2016)
[18] J. B. Cheng, S. Y. Li, Y. R. Liu *et al.*, Phys. Rev. D **101**(11), 114017 (2020)
[19] M. Karliner and J. L. Rosner, arXiv:2008.05993 [hep-ph]
[20] J. R. Zhang, arXiv:2008.07295 [hep-ph]
[21] X. G. He, W. Wang, and R. Zhu, arXiv:2008.07145 [hep-ph]
[22] H. X. Chen, W. Chen, R. R. Dong *et al.*, arXiv:2008.07516 [hep-ph]
[23] Q. F. Lu, D. Y. Chen and Y. B. Dong, arXiv:2008.07340 [hep-ph]
[24] F. K. Guo and U. G. Meissner, Phys. Rev. D **84**, 014013 (2011)
[25] R. Molina, T. Branz, and E. Oset, Phys. Rev. D **82**, 014010 (2010)
[26] X. H. Liu, M. J. Yan, H. W. Ke *et al.*, arXiv:2008.07190 [hep-ph]
[27] M. Z. Liu, J. J. Xie, and L. S. Geng, arXiv:2008.07389 [hep-ph]
[28] M. W. Hu, X. Y. Lao, P. Ling *et al.*, arXiv:2008.06894 [hep-ph]
[29] J. He, Phys. Rev. D **92**(3), 034004 (2015)
[30] P. L. Lu and J. He, Eur. Phys. J. A **52**(12), 359 (2016)
[31] R. Molina and E. Oset, Phys. Rev. D **80**, 114013 (2009)

[32] M. C. Birse, Z. Phys. A **355**, 231-246 (1996)
[33] F. Aceti, M. Bayar, E. Oset *et al*., Phys. Rev. D **90**(1), 016003 (2014)
[34] H. Y. Cheng, C. Y. Cheung, G. L. Lin *et al*., Phys. Rev. D **47**, 1030-1042 (1993)
[35] T. M. Yan, H. Y. Cheng, C. Y. Cheung *et al*., Phys. Rev. D **46**, 1148-1164 (1992)
[36] M. B. Wise, Phys. Rev. D **45**(7), 2188 (1992)
[37] R. Casalbuoni, A. Deandrea, N. Di Bartolomeo *et al*., Phys. Rept. **281**, 145-238 (1997)
[38] G. J. Ding, Phys. Rev. D **79**, 014001 (2009)
[39] R. Chen, Z. F. Sun, X. Liu *et al*., Phys. Rev. D **100**(1), 011502 (2019)
[40] Y. R. Liu and M. Oka, Phys. Rev. D **85**, 014015 (2012)
[41] C. Isola, M. Ladisa, G. Nardulli *et al*., Phys. Rev. D **68**, 114001 (2003)
[42] A. F. Falk and M. E. Luke, Phys. Lett. B **292**, 119-127 (1992)
[43] X. K. Dong, Y. H. Lin, and B. S. Zou, Phys. Rev. D **101**(7), 076003 (2020)
[44] J. He, Y. Liu, J. T. Zhu *et al*., Eur. Phys. J. C **80**(3), 246 (2020)
[45] A. Matsuyama, T. Sato, and T. S. H. Lee, Phys. Rept. **439**, 193-253 (2007)
[46] M. Bando, T. Kugo, and K. Yamawaki, Phys. Rept. **164**, 217-314 (1988)
[47] G. Janssen, K. Holinde, and J. Speth, Phys. Rev. C **49**, 2763-2776 (1994)
[48] D. Ronchen, M. Doring, F. Huang *et al*., Eur. Phys. J. A **49**, 44 (2013)
[49] J. He, H. Huang, D. Y. Chen *et al*., Phys. Rev. D **98**(9), 094019 (2018)
[50] J. He, Phys. Rev. D **95**(7), 074031 (2017)
[51] J. He, Phys. Rev. C **91**(1), 018201 (2015)
[52] J. He, Phys. Lett. B **753**, 547-551 (2016)
[53] J. He, Eur. Phys. J. C **79**(5), 393 (2019)
[54] J. He and D. Y. Chen, Eur. Phys. J. C **79**(11), 887 (2019)
[55] H. Y. Cheng, C. K. Chua, and A. Soni, Phys. Rev. D **71**, 014030 (2005)
[56] F. Gross and A. Stadler, Phys. Rev. C **82**, 034004 (2010)
[57] J. He, D. Y. Chen, and X. Liu, Eur. Phys. J. C **72**, 2121 (2012)
[58] J. He and X. Liu, Eur. Phys. J. C **72**, 1986 (2012)
[59] J. He and P. L. Lu, Int. J. Mod. Phys. E **24**(11), 1550088 (2015)
[60] J. R. Taylor, Scattering Theory: The Quantum Theory on Nonrelativistic Collisions (John Wiley & Sons,Inc., New York, 1972)
[61] R. Molina and E. Oset, Phys. Lett. B **811**, 135870 (2020)
[62] J. J. Qi, Z. Y. Wang, Z. F. Zhang *et al*., [arXiv:2101.06688 [hep-ph]]
[63] L. S. Geng and E. Oset, Phys. Rev. D **79**, 074009 (2009)
[64] R. Molina, H. Nagahiro, A. Hosaka *et al*., Phys. Rev. D **80**, 014025 (2009)